Mon. Not. R. Astron. Soc. **360,** 60–68 (2005) doi:10.1111/j.1365-2966.2005.08883.x

The elliptical galaxy colour–magnitude relation as a discriminant between the monolithic and merger paradigms

S. Kaviraj,[1⋆] J. E. G. Devriendt,[1,2] I. Ferreras[1,3] and S. K. Yi[1]

[1]*Department of Physics, University of Oxford, Keble Road, Oxford OX1 3RH*
[2]*Observatoire Astronomique de Lyon, 9 Avenue Charles André, 69561 Saint-Genis Laval, France*
[3]*Department of Physics, Institute of Astronomy, ETH Hoenggerberg HPF D8, 8093 Zurich, Switzerland*

Accepted 2005 January 28. Received 2005 January 26; in original form 2004 January 9

ABSTRACT

The colour–magnitude relation (CMR) of cluster elliptical galaxies has been widely used to constrain their star formation histories (SFHs) and to discriminate between the monolithic collapse and merger paradigms of elliptical galaxy formation. We use a Λ cold dark matter hierarchical merger model of galaxy formation to investigate the existence and redshift evolution of the elliptical galaxy CMR in the merger paradigm. We show that the SFH of cluster ellipticals predicted by the model is *quasi-monolithic*, with only $\sim$10 per cent of the total stellar mass forming after $z \sim 1$. The quasi-monolithic SFH results in a predicted CMR that agrees well with its observed counterpart in the redshift range $0 < z < 1.27$. We use our analysis to argue that the *elliptical-only* CMR can be used to constrain the SFHs of present-day cluster ellipticals only if we believe a priori in the monolithic collapse model. It is not a meaningful tool for constraining the SFH in the merger paradigm, since a progressively larger fraction of the progenitor set of present-day cluster ellipticals is contained in late-type star-forming systems at higher redshift, which cannot be ignored when deriving the SFHs. Hence, the elliptical-only CMR is not a useful discriminant between the two competing theories of elliptical galaxy evolution.

Key words: galaxies: elliptical and lenticular, cD – galaxies: evolution – galaxies: formation – galaxies: fundamental parameters.

1 INTRODUCTION

Evolution with redshift of fundamental physical relations can provide robust constraints on the epoch of formation and subsequent evolution of early-type galaxies. The apparently universal relationship between colour and luminosity of elliptical galaxies, usually referred to as the *colour–magnitude relation* (CMR), was first established by Sandage & Vishvanathan (1977), although the correlation between these two quantities had been demonstrated before (e.g. Baum 1959; de Vaucouleurs 1961; McClure & van den Bergh 1968). The observed CMR has been widely used as a discriminant between the two competing theories of early-type galaxy evolution, the monolithic collapse model (e.g. Larson 1974; Kodama & Arimoto 1997) and the hierarchical merger model (e.g. Kauffmann, White & Guiderdoni 1993; Somerville & Primack 1999; Cole et al. 2000; Hatton et al. 2003; Khochfar & Burkert 2003).

A comprehensive study of the CMR, using photometric data based on charge-coupled device (CCD) observations of the nearby Virgo and Coma clusters, was first undertaken by Bower, Lucey & Ellis (1992, hereafter BLE92). Their results showed a remarkably small scatter about the mean relation. Their interpretation of the results, in the context of the *monolithic collapse model*, was to attribute the slope of the CMR to a variation in mean metallicity with luminosity and to attribute the small scatter to a small age dispersion between galaxies of the same size. They concluded that the epoch of formation of elliptical galaxies should be at $z > 2$. Subsequent studies of the CMR extended the BLE92 results to intermediate redshifts ($0 < z < 1$) and showed that there was no detectable evolution of the slope and scatter with time (e.g. Ellis et al. 1997; Stanford, Eisenhardt & Dickinson 1998; Gladders et al. 1998; van Dokkum et al. 2000). The results from these studies were interpreted as confirmation of a high-redshift formation epoch of cluster ellipticals followed by passive evolution to present day.

Subsequent studies indicated that the key characteristics of the CMR (slope and scatter) that were derived by these authors needed some modification. Elliptical galaxies commonly display radial colour gradients (e.g. de Vaucouleurs 1961; Sandage & Vishvanathan 1978; Franx, Illingworth & Heckman 1989; Peletier et al. 1990), being optically redder at their cores than at the outskirts. Galaxy colours in the majority of these CMR studies were derived using *fixed apertures*, which, given that a galaxy's intrinsic size may vary, meant sampling different portions of different galaxies. Accounting for the effect of fixed-aperture photometry is essential in

⋆E-mail: skaviraj@astro.ox.ac.uk

the context of this study. Our aim is to reproduce the properties of the observed optical CMR using a hierarchical merger model from low to high redshift. However, since our model lacks spatial information on the scale of galaxies, producing a *central* CMR is not possible within the model, and we must, therefore, compare our results to aperture-corrected photometry.

Numerous authors have attempted to quantify the *fixed-aperture bias* that may result as a result of the presence of colour gradients. An efficient way to control this effect is to measure the colour inside an aperture that scales with the size of the galaxy (e.g. Bower, Kodama & Terlevich 1998; Terlevich, Caldwell & Bower 2001; Scodeggio 2001), such that one samples an identical fraction of the light in each galaxy. Bower et al. (1998) compared the CMR slope observed by BLE92 with the slope derived after replacing a fixed aperture with the parameter D_v – the size of the galaxy within which the mean surface brightness is 19.80 mag arcsec^{-2}. They estimated that colour gradients accounted for roughly 30 per cent of the slope, i.e. the magnitude of the slope in the D_v CMR was roughly two-thirds of that derived using fixed apertures in BLE92. Crucially, their study indicated that the CMR maintains a *significant slope* even after correcting for colour gradients. A series of other studies have also studied the effect of removing the fixed-aperture bias. Shallower CMR slopes have been reported by Prugniel & Simien (1996), who used colours derived within the *effective radius* R_e (the radius that contains half the galaxy's light), and by Fioc & Rocca-Volmerange (1999), who used total magnitudes and colours. Scodeggio (2001) suggested that recomputing colours over R_e for the BLE92 galaxies causes the apparent slope to decrease from -0.082 ± 0.008 to -0.016 ± 0.018, a value that is statistically consistent with a zero slope. In addition, the scatter increases from 0.035 to 0.136, because of the large intrinsic scatter in the colour gradients. However, the uncertainty in colour measurements within R_e can be significantly larger than within D_v, because the surface brightness within D_v is higher. At 2σ the Scodeggio (2001) data are consistent with slopes between $+0.02$ and -0.52. Modifying the BLE92 slope for colour gradients, using the 30 per cent correction factor derived by Bower et al. (1998), gives -0.054, so that within the errors there is agreement between the various studies [see also Bernardi et al. (2003), who derive optical CMRs from 9000 early-type galaxies drawn from the SDSS].

Over the past decade, there has been steadily accumulating evidence for morphological evolution amongst cluster galaxies, which suggests that formation mechanisms of cluster ellipticals are at least *not uniquely monolithic*. Although approximately 80 per cent of galaxies in the cores of present-day clusters have early-type morphologies (Dressler 1980), a higher fraction of spiral galaxies have been reported in clusters at $0.3 < z < 0.8$ (e.g. Butcher & Oemler 1984; Dressler et al. 1997; Couch et al. 1998; van Dokkum et al. 2000), along with increased rates of merger and interaction events (e.g. Couch et al. 1998; van Dokkum et al. 1999). Kauffmann, Charlot & White (1996) suggested that only approximately one-third of early-type galaxies in the Canada–France Redshift Survey (CFRS, Schade et al. 1995) were fully formed and evolving passively. Franceschini et al. (1998) found a remarkable absence of early-types galaxies at $z > 1.3$ in a K-band selected sample in the *Hubble Deep Field*. These results strongly suggest that early-type galaxies in nearby and distant clusters may have been formed from late-type progenitors (e.g. Butcher & Oemler 1984; Dressler et al. 1997) and highlight the possible if not essential role of merger and interaction events in the formation of early-type galaxies. In particular, if the merger paradigm is correct, then late-type progenitors of the present-day cluster ellipticals must be included in any method (e.g. the CMR) employed to determine their star formation histories (SFHs). Excluding these late-type progenitors would produce a distorted view of their formation histories (progenitor bias), a point first suggested and explored in detail by van Dokkum & Franx (2001).

Given the accumulating evidence for formation of early-type galaxies from star-forming progenitors at fairly recent epochs, a number of authors have successfully reconciled the observed CMR with galaxy merging models (Kauffmann & Charlot 1998; Bower et al. 1998; Shioya & Bekki 1998; van Dokkum et al. 1998). Apart from Kauffmann & Charlot (1998), these studies have not involved a fully realistic semi-analytical galaxy formation model that incorporates the important effects of galaxy merging on the chemo-photometric evolution of galaxies. One of our aims is to extend these studies by applying a ΛCDM hierarchical merger model to study the CMR from low to high redshift.

We begin our study by discussing the comparative effects of age and metallicity in determining the model $(U - V)$ CMR at the present day and tracing the bulk SFHs of cluster ellipticals as a function of redshift. We then explore the predicted evolution of the CMR to high redshifts, compare with existing observational evidence and, in particular, quantify the effect of progenitor bias. Using our analysis of progenitor bias, we present arguments to show that the commonly used *elliptical-only* CMR, even when it is derived using equal light fractions (cf. Bower et al. 1998; Terlevich et al. 2001; Scodeggio 2001), can only be used to constrain the SFHs of cluster ellipticals *if we believe a priori in a monolithic collapse model*. It is not a meaningful method of constraining the SFH in the hierarchical merger picture. Hence it is also not a useful discriminant between the two competing theories of galaxy evolution.

2 MODEL PARAMETERS THAT AFFECT THE PRESENT-DAY CMR

The model we use in this study is GALICS, which combines large-scale N-body simulations with simple analytical recipes for the dynamical evolution of baryons within dark matter (DM) haloes. We direct readers to Hatton et al. (2003) for specifics regarding the model. There are certain key parameters in the model that affect the age and metallicity of the model galaxies and thus have an impact on the slope, scatter and absolute colour of the predicted CMR. A discussion of these model parameters is necessary, not only to elucidate their effect on the CMR, but also because the actual setup we use in this study is slightly different from the reference model given in Hatton et al. (2003). The setup has been altered, first to make some corrections to the metallicity of fresh gas injected into DM haloes, and secondly to bring the predicted metallicities of the model galaxies into agreement with current observational evidence. Table 1 summarizes the changes in the characteristics of the CMR due to variations in these parameters. We note that fiducial predictions of the GALICS model, presented in Hatton et al. (2003), such as the galaxy luminosity function, Tully–Fisher relation and Faber–Jackson relation, remain unchanged under this modified setup. In the subsequent sections we present an explanation of the parameters and the values used in this study.

2.1 Baseline metallicity

The reference model in Hatton et al. (2003) adds *pristine*, i.e. metal-free, gas to DM haloes when they are identified. However, the haloes are not identified until they achieve a threshold mass of $10^{11}\,M_\odot$. In reality, early Population II stars would already have polluted the interstellar medium (ISM) in the time that it takes for such halo

identifications to take place. Hence, the gas in the haloes should not be pristine but *slightly polluted*. Chemical enrichment models (e.g. Devriendt, Guiderdoni & Sadat 1999) suggest that this pollution should be of the order of $0.1\,Z_{\odot}$. Hence, we use this value as a *baseline metallicity* for fresh gas injected into DM haloes in the model. The baseline metallicity has a negligible impact on the slope and scatter of the CMR but slightly affects the absolute colour of the cluster sample, as it changes the average metallicities of the model galaxies.

2.2 Black hole threshold mass and initial mass function

Another parameter that affects the metal input into the ISM, and therefore the average metallicity of the stellar population, is the threshold mass at which a star becomes a black hole. The formation of a black hole removes material (including metals) from the surroundings – thus a lower threshold mass allows more stars to form black holes and reduces the overall metal enrichment of the ISM. The black hole threshold mass (BHT) is still poorly understood, but estimates suggest masses around $50 \pm 10\,M_{\odot}$ (Tsujimoto et al. 1997), based on a combination of local stellar [O/Fe] abundances and chemical enrichment analysis. We use a black hole threshold mass of $60\,M_{\odot}$ in this study.

Since massive stars make a significant contribution to the metal enrichment of the ISM, the proportion of massive stars and hence the initial mass function (IMF) affect the mean metallicities of the model galaxies. In this study we use a Kennicutt IMF (Kennicutt 1983), which was also used in the fiducial model of Hatton et al. (2003). Both the BHT and IMF increase the dynamical metal enrichment of the ISM. This changes not only the mean metallicity of the galaxies, and hence their absolute colour, but also makes the slope of the CMR steeper. This is because more massive galaxies, which have deeper potential wells, retain gas and therefore metals more effectively, leading to higher enrichment of the ISM and stellar populations that are born from it. However, less massive galaxies tend to lose their gas content anyway, so that a larger injection of metals into their ISM does not have a big impact on the metallicity of their stellar populations. As a result of this differential behaviour, the slope of the CMR becomes steeper.

3 PROPERTIES OF PRESENT-DAY CLUSTER ELLIPTICALS

In this section, we explore the present-day CMR predicted by our model. Fig. 1 presents the predicted CMR in our model for cluster ellipticals at $z = 0$. Also shown is a linear least-squares fit to the points (dashed line) and a progressive one-sigma fit to the sample, with the error bars indicating the local spread of points about the best-fitting relation. We select present-day cluster ellipticals by identifying elliptical galaxies in DM haloes with masses of $10^{14}\,M_{\odot}$ and above. Also shown in Fig. 1 is the CMR sequence with galaxies coded according to their mean metallicities and ages. The bottom panel splits the model ellipticals into their individual clusters. The model slope is derived in all cases using a linear least-squares fit. The scatter is calculated using Tukey's bi-weight statistic (Beers, Flynn & Gebhardt 1990), which has commonly been used by observers in CMR studies. Table 1 compares the model CMR with those derived by BLE92 and Bower et al. (1998) within $D_{\rm v}$ and by Scodeggio (2001) using the effective radius $R_{\rm e}$.

The predicted model slope is consistent with both the value reported by Scodeggio (2001) and the BLE92 value, after correcting for colour gradients using the 30 per cent correction derived in

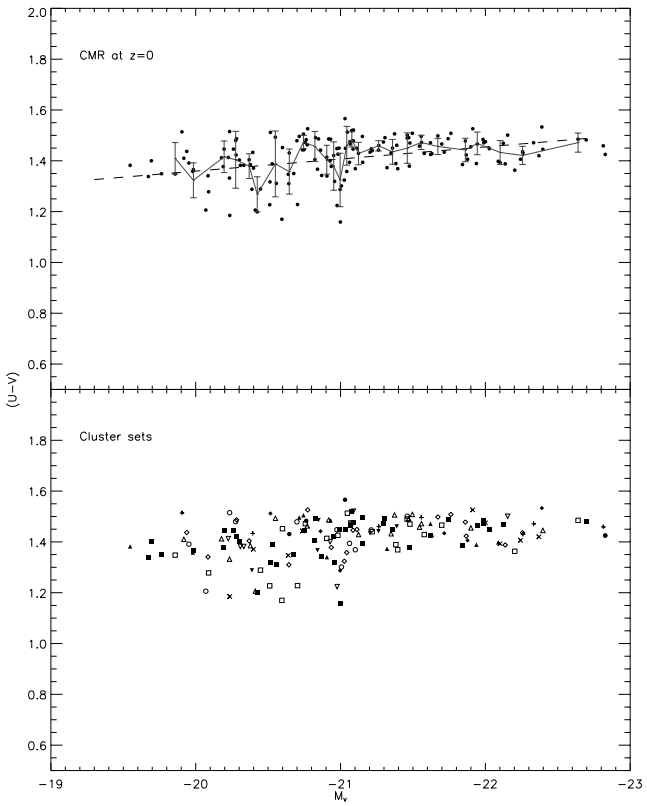

Figure 1. The model colour–magnitude relation at $z = 0$. Top: CMR sequence with a linear least-squares fit (dotted line) and a progressive one-sigma fit to the sample. Bottom: Cluster ellipticals split into their individual clusters.

Bower et al. (1998). The predicted scatter is smaller than that derived by Scodeggio (2001) but roughly 1.5 times larger than that reported by Bower et al. (1998). We note, however, that the scatter in the model galaxies itself varies from cluster to cluster, so that the intracluster scatter may be different from the global value across all clusters. In Fig. 2 we split our sample of model ellipticals into their respective clusters and plot the intracluster scatter as a fraction of the global scatter in the sample. We find, for example, that the cluster with the largest number of ellipticals has a lower scatter than the global value, although there are other large clusters that exhibit a scatter above the global value. We note that our model galaxy sample is an ensemble of galaxy sets from different clusters, whereas the observations usually refer to only one cluster. There may be additional issues contributing to the discrepancy between the model and observed scatter – for example, there appear to be strong radial colour gradients in cluster populations at low redshift (e.g. Margoniner et al. 2001; Ellingson et al. 2001; Pimbblet et al. 2002; De Propris et al. 2004), such that bluer objects reside in the outer parts of clusters. The scatter of the observed CMR would therefore depend on the maximum cluster-centric radius sampled in the observations. In addition, since the observations are not derived from total colours, it is possible that colour gradients are correlated with deviations from the true total-colour CMR in such a way that aperture colours appear to have smaller scatter. For these reasons, we do not find the discrepancy between the model and observed scatters particularly compelling.

We find that the model predicts a significant correlation between colour and luminosity. An important question is *how* the model CMR

Table 1. Variations in CMR slope and scatter with baseline metallicity, initial mass function (IMF) and black hole threshold mass (BHT). The slope is derived from least-squares fits (over the magnitude range $M_V = -19$ to $M_V = -23$) and the scatter is calculated using Tukey's bi-weight statistic. The values in bold indicate the parameters used for this study.

Baseline metallicity ($Z_\odot$)	Initial mass function (IMF)	Black hole threshold mass (BHT) 45 $M_\odot$	60 $M_\odot$	120 $M_\odot$
0	Kennicutt	-0.037 ± 0.007 0.072	-0.049 ± 0.007 0.079	-0.050 ± 0.009 0.094
0	Scalo	-0.034 ± 0.006 0.057	-0.033 ± 0.009 0.070	-0.047 ± 0.010 0.10
0.1	Kennicutt	-0.036 ± 0.009 0.075	$\mathbf{-0.047 \pm 0.010}$ **0.082**	-0.052 ± 0.010 0.12
0.1	Scalo	-0.032 ± 0.007 0.061	-0.034 ± 0.010 0.078	-0.045 ± 0.010 0.10

Table 2. Comparison between the characteristics of our model CMR at $z = 0$ with BLE92, *corrected for colour gradients using the 30 per cent correction* given in Bower et al. (1998) and Scodeggio (2001), who used the effective radius (R_e) of galaxies to derive colours. For the model CMR, the slope is derived from least-squares fits (over the magnitude range $M_V = -19$ to $M_V = -23$) and the scatter is calculated using Tukey's bi-weight statistic.

Source	Slope	Scatter (mag)	Colour
Bower et al. (1992, 1998) (Coma)	-0.054 ± 0.007	0.049	$U - V$ (within D_v)
Scodeggio (2001) (Coma)	-0.016 ± 0.018	0.136	$U - V$ (within R_e)
This study	-0.047 ± 0.010	0.082	$U - V$ (total magnitudes)

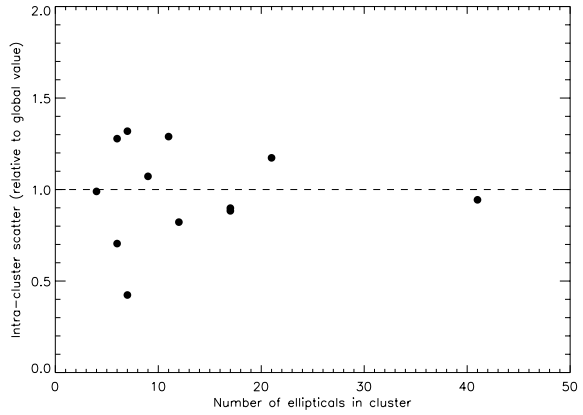

Figure 2. Intracluster scatter as a fraction of the total scatter plotted against the elliptical occupancy of each cluster.

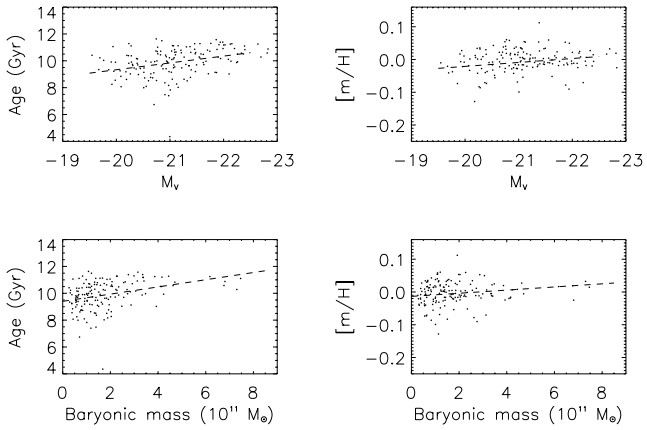

Figure 3. Variation of mass-weighted average ages and metallicities with absolute V-band luminosity and baryonic mass.

is generated at the present day. Clearly, in a hierarchical merger scenario, age is expected to play a part in generating any such sequence. It is therefore crucial to disentangle the effects of age and metallicity and to determine how much of the correlation is generated by a variation in age and how much by a variation in metallicity with luminosity.

Fig. 3 shows the variation in the mean ages and metallicities of the model cluster ellipticals with absolute V-band luminosity. We also show the age–metallicity parameter space for these model galaxies in Fig. 4. We should note here that the metallicity resolution in the model is low, with stellar mass resolved only into five metallicity bins in the range $-1.3 < [m/\mathrm{H}] < 0.5$. We have indicated the *maximum* average metallicity error for model galaxies with subsolar and supersolar metallicities in Fig. 4, by considering the half-widths of our metallicity bins. The resolution in age, by comparison, is extremely good (0.1 Gyr), as indicated by the small age error bars.

The model predicts a gradient in both the age–luminosity and metallicity–luminosity relations, so that larger ellipticals are both older and more metal-rich. We note first that, contrary to previous studies (e.g. Kauffmann & Charlot 1998), higher-mass (-luminosity) ellipticals are predicted to have *larger* mean ages, in agreement with observational evidence (see e.g. Trager et al. 2000a,b; Caldwell, Rose & Concannon 2003). Current understanding of cooling flows in clusters is poor. Models suggest that, if large inflows of cold gas are allowed at the centre of virialized DM haloes, it is impossible to prevent a large fraction of this material from forming stars (e.g. Cole et al. 2000), which are not observed at the present epoch. To prevent this, one has to *reheat or keep gas hot* in massive

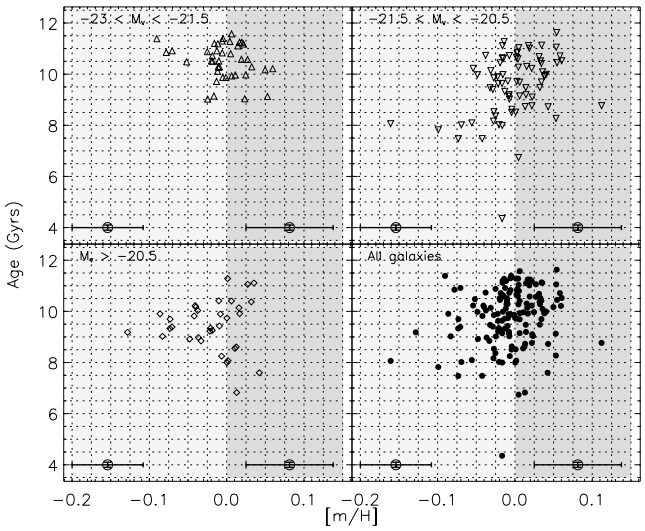

Figure 4. Age–metallicity parameter space in model cluster ellipticals split into luminosity classes. Upper left: High-luminosity model ellipticals ($-23.0 < M_V < -21.5$). Upper right: Intermediate-luminosity model ellipticals ($-21.5 < M_V < -20.5$). Lower left: Low-luminosity model ellipticals ($M_V > -20.5$). Lower right: All model ellipticals. The horizontal error bar shows the *maximum* average metallicity error for model galaxies with subsolar and supersolar metallicities, calculated by considering the half-widths of the metallicity bins in the model. The vertical error bar shows the maximum error in the ages the model ellipticals.

DM haloes. Various authors have tackled this problem in different ways. Kauffmann et al. (1993), for instance, prevented cooling from taking place in DM haloes with circular velocities of 350 km s^{-1} and above. GALICS takes advantage of the observed correlation between active galactic nuclei (AGN) and bulge mass (Magorrian et al. 1998) and assumes that AGNs are efficient enough to halt cooling flows completely as soon as the bulge that harbours them reaches a critical mass of 10^{11} M$_{\odot}$. This coupling between AGN feedback and bulge mass prevents star formation early enough in large elliptical galaxies to allow them to grow solely through mergers of gas-poor progenitors. Thus, although galaxies with a larger mass experience their last merging events at a later time than their less luminous counterparts, the small gas fraction at these last-merger epochs prevents any substantial production of young stars from merger-driven starbursts. Therefore, although more massive galaxies are *dynamically younger* based on their *merger record*, their stellar populations are, nevertheless, *older*. The average predicted age of a cluster elliptical is approximately 9.8 Gyr, and the scatter in age increases towards the low-mass end, in agreement with recent observational studies in clusters such as Virgo (Caldwell et al. 2003). The average metallicity is approximately solar and the gradient in metallicity is modest, also in general agreement with recent spectroscopic studies of nearby cluster environments (Caldwell et al. 2003).

A comparison with simple stellar population (SSP) models (Yi 2003) shows that roughly half of the CMR slope is generated by the age–luminosity gradient, with the rest attributable to the metallicity–luminosity gradient in the model sample. Clearly, the age and metallicity gradients *complement* each other in this model, in contrast to Kauffmann & Charlot (1998) where the *anticorrelation* between age and luminosity required a large compensating metallicity gradient (generated through high metal yields) to produce a CMR that was consistent with the BLE92 observations.

It is clearly beyond the scope of this paper to make a detailed comparison of how feedback is treated in GALICS and the specific model of Kauffmann & Charlot (1998). However, we note that there are at least two main differences:

(i) Cosmological models – Kauffmann & Charlot (1998) adopt the SCDM cosmology while GALICS adopts the ΛCDM cosmology.

(ii) GALICS derives feedback directly from the mass locked up in the spheroidal component of the galaxy, while Kauffmann & Charlot (1998) use the velocity dispersion in DM haloes alone to stop the cooling.

The first point implies that, in GALICS, structures of a given mass will be assembled earlier on average than in Kauffmann & Charlot (1998). The second point means that gas does not cool onto a spiral galaxy which sits in a halo with circular velocity greater than or equal to 350 km s^{-1} in the Kauffmann & Charlot (1998) model whereas it does in GALICS, provided the spiral does not possess a massive bulge. Feedback in GALICS is explicitly linked to the mass buildup of spheroids, which in turn is correlated to the mass (velocity dispersion) buildup of the host DM halo. However, this latter correlation need not be linear, since the mass buildup of spheroids depends on local physics (e.g. disc instabilities and mergers). We attribute the differences in the results of Kauffmann & Charlot (1998) and GALICS to these two factors (cosmology and feedback modelling), but note that there may be other factors in the details of the modelling that might cause discrepancies in the relationship between age, metallicity and luminosity in these two models.

Fig. 5 presents the bulk cumulative SFH of the model cluster ellipticals. The SFH is shown both split into the five GALICS metallicity bins and considering all stellar mass. The cumulative SFH shows that ∼10 per cent of the total stellar mass (solid line) was formed after $z = 1$, with ∼65 per cent and ∼40 per cent already in place at $z = 2$ and $z = 3$, respectively. The bulk SFH is quasi-monolithic because the low cold gas fraction at low redshifts ($z < 1$) means that merger-driven star formation does not produce substantial amounts of stellar material. This enables the model elliptical CMR to maintain its slope and small scatter up to high redshifts (Section 4).

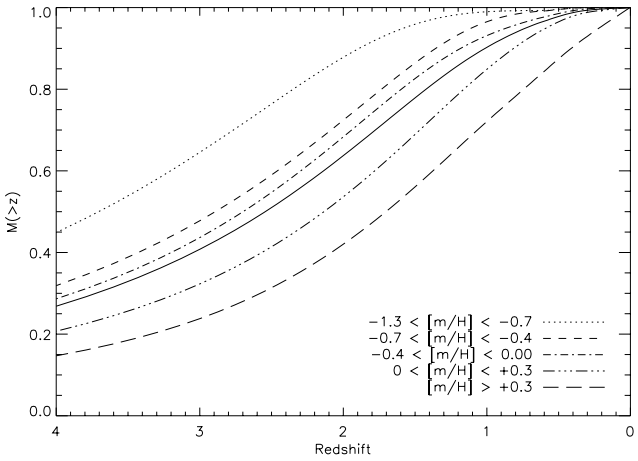

Figure 5. Stellar mass fraction formed *at or before* a given redshift. The solid line shows the cumulative mass fraction for all stellar mass. The other curves represent stellar mass in five different metallicity ranges.

4 EVOLUTION OF THE CMR WITH REDSHIFT

We now check if it is possible to reconcile the model CMR with observational data at various redshifts. Fig. 6 shows the predicted evolution of the model CMR from the present day to a redshift of 1.27, which is roughly the redshift limit of current observational evidence on early-type cluster galaxies (van Dokkum et al. 2001). As before, the dashed line displays a linear least-squares fit and we also show a progressive one-sigma fit to the sample, with the error bars indicating the local spread of points about the best-fitting relation. Fig. 7 traces the evolution of the slope and the scatter. The shaded region denotes the area enclosed by the predicted slopes and their associated errors.

We note that the definition of a cluster elliptical will change with increasing redshift. We assumed in our analysis of present-day cluster ellipticals that DM haloes with a mass equal to or greater than $10^{14}\,M_{\odot}$ host regions of highest baryonic density and therefore galaxy clusters. However, since DM haloes are being steadily formed through time, maintaining a hard mass cut-off of $10^{14}\,M_{\odot}$ for all redshifts would not be correct. To make this definition consistent with changing redshift, we take into account the accretion history of DM haloes in the model. We first compute an average accretion history of the present-day DM haloes with masses of $10^{14}\,M_{\odot}$ and above as a function of redshift. At each redshift we then define a *cluster hosting DM halo* as one whose mass is equal to or exceeds the value given by the average accretion history. We note that our values are consistent with van den Bosch (2002), who provides theoretical prescriptions for computing universal DM mass accretion histories.

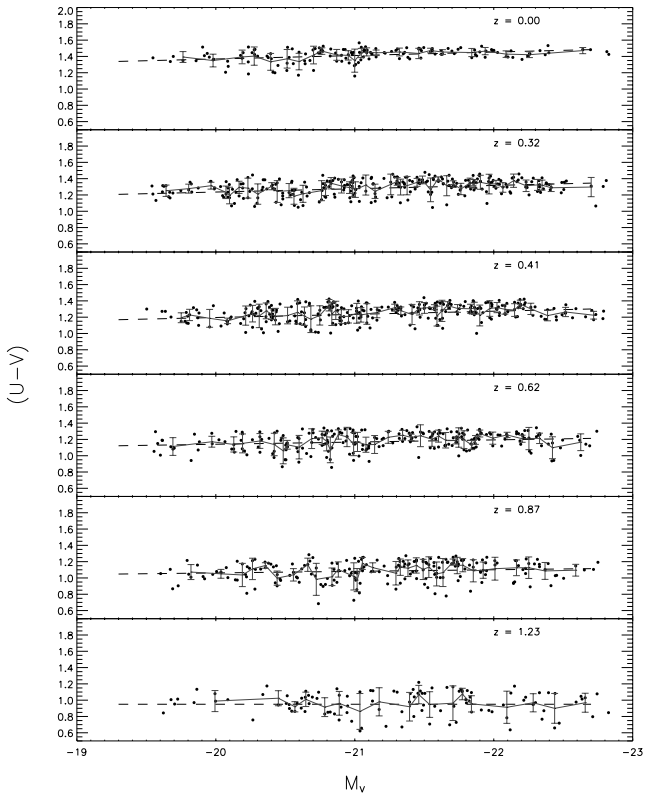

Figure 6. Predicted redshift evolution of the model CMR from the present day to $z = 1.23$, which is roughly the redshift limit of current observational evidence on early-type cluster galaxies. Also shown is a linear least-squares fit (dotted line) and a progressive one-sigma fit, with the error bars indicating the local spread of points about the mean relation.

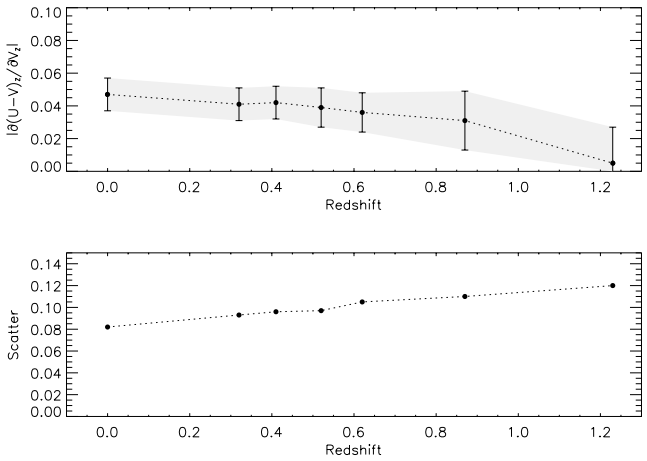

Figure 7. Redshift evolution of the slope and scatter in the model $(U - V)$ versus V CMR. Although the evolution in the slope is zero within the errors in the range $0 < z < 0.8$, the change in the slope from the value at the present day becomes appreciable at $z = 1.23$.

We see from Fig. 7 that there is gradual evolution in the CMR slope, although in the range $0 < z < 0.8$ the evolution in the slope is zero within the errors. However, once we move out to $z = 1.23$ the change in slope is appreciable compared to the value at the present day. Within the errors, we see that at high redshifts (e.g. $z = 1.23$) the CMR loses any detectable slope, partly because the expected increase in the scatter masks any correlation that may be present.

In Fig. 8 we put the evolution of the predicted CMR in the context of observational evidence. We use a variety of sources that have explored the CMR in various colours. We apply the 30 per cent correction for colour gradients derived by Bower et al. (1998) to studies that have used fixed apertures. We find that the slopes of the model and observed CMRs match well within the errors at all redshifts. In particular, we note that van Dokkum et al. (2001) reported a slope at $z = 1.27$ that was significantly lower than the BLE92 value at the present day. This suggests that the CMR slope does indeed decrease, in agreement with the expectations of a hierarchical merger scenario. The values for the model scatter are also fairly consistent with the observations, given the previous discussion in Section 2 regarding possible reasons for the discrepancy between the model and observed scatter at $z = 0$. However, we should note that the *tightness* of the predicted CMR (especially at the high-luminosity end) seems larger than what appears in observational studies. The model ellipticals do occupy the *red* part of the sequence (shaded region in Fig. 8), with a scatter to bluer colours which increases with redshift. However, comparing our results at $z \sim 0.8$ to, for example, (van Dokkum et al. 2000, Fig. 8), we find that, at comparable redshift, the observed elliptical CMR is tighter than our model predictions, although outliers do exist in the observed elliptical sample.

5 PROGENITOR BIAS

When comparing the slope and scatter of the CMR at various redshifts, we should ideally sample the *same stellar mass at every redshift*. Only then are the slope and scatter truly meaningful tracers of the star formation history of the *daughter* mass seen today. However, an unavoidable result of the merger paradigm is that, since early-type systems form through the amalgamation of late-type units, a progressively *larger* fraction of the stellar mass we see today in cluster ellipticals is locked up in late-type (spiral and irregular) units at higher redshifts. Hence the early-type systems at high

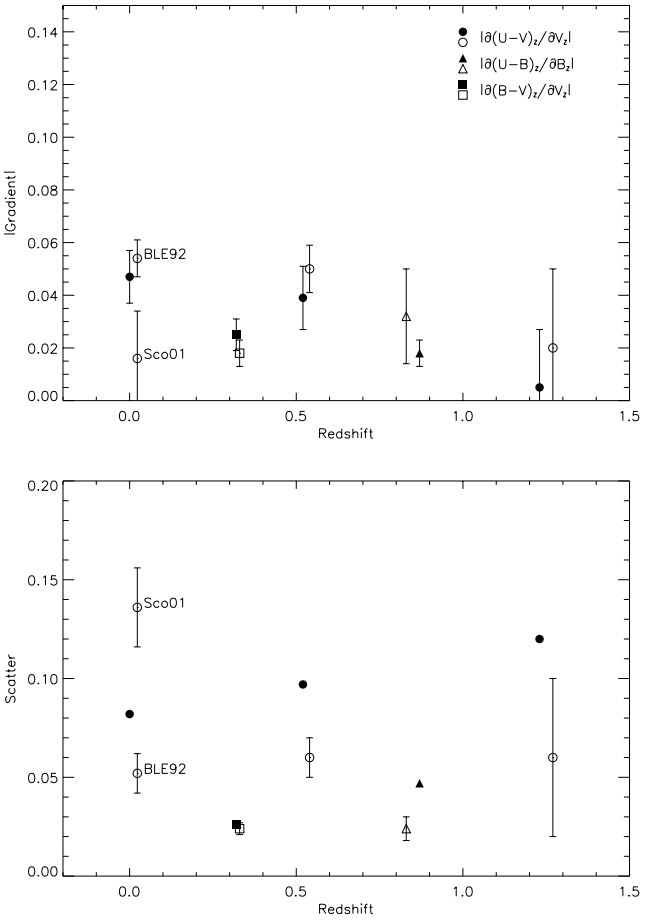

Figure 8. CMR evolution with redshift. Note that we show the properties of CMRs in *three different colours* as given in the relevant studies: $(U-V)$ data are marked as circles, $(U-B)$ data are shown as triangles, and $(B-V)$ data are shown as squares. Filled symbols represent model values and open symbols represent observational results. We apply the 30 per cent correction for colour gradients derived by Bower et al. (1998) to studies that have used fixed apertures. The observational data from left to right are taken from: Bower et al. (1992) (marked BLE92), Scodeggio (2001) (marked Sco01), van Dokkum et al. (1998), Ellis et al. (1997), van Dokkum et al. (2000) and van Dokkum et al. (2001). We do not transform all results to a single colour because this requires an assumption of the template used to perform the transformation, which may introduce additional uncertainties into the comparison.

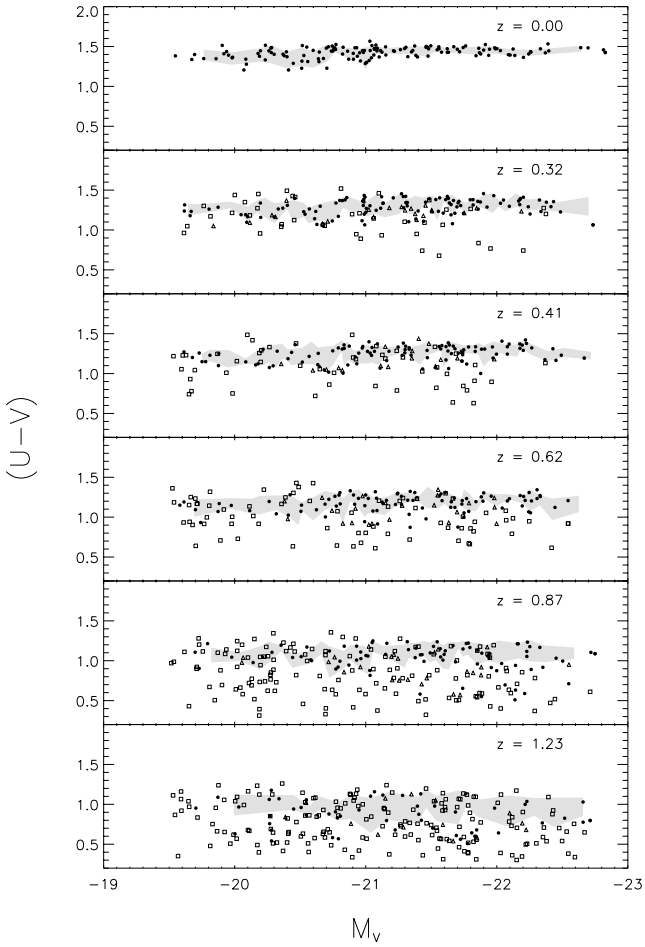

Figure 9. Progenitor bias: filled circles are ellipticals, open triangles are S0s, and open squares are late-type systems (spirals and irregulars). All galaxies are progenitors of the galaxies at $z = 0$. The shaded region indicates the mean *elliptical-only* relation and its associated errors taken from Fig. 6.

redshift form a progressively narrower subset of the progenitors of present-day elliptical systems. Consequently, by not taking into account these late-type progenitors, we introduce a bias in the CMR, mainly in terms of the observed scatter. In this section we quantify the effect of this *progenitor bias* (see also van Dokkum et al. 2001). Although tracing an astronomical object back through time is impossible observationally, it becomes a simple exercise within the model.

In Fig. 9 we restrict ourselves to the *progenitor set* of present-day cluster ellipticals. We show only those galaxies (regardless of morphology) that eventually contribute to the formation of cluster ellipticals that exist at $z = 0$. We are therefore tracing the *same stellar mass* back through time, regardless of the type of system that hosts it. We find that including progenitors with S0 morphology does not change the slope of the CMR. The overall scatter increases slightly at higher redshifts ($z > 0.62$), although the elliptical-only scatter agrees, within errors, with the E+S0 scatter. S0s, however, tend to contribute more outliers to the CMR at higher redshifts. Including the late-type progenitors causes the scatter to increase approximately three-fold in the range $z > 0.8$, compared to the elliptical-only scenario. This result agrees with CMR observations at high redshift. For example, van Dokkum et al. (2000) found that the elliptical CMR at $z = 0.83$ has a scatter of $\sim$0.024 while the scatter for all morphological types is $\sim$0.081 – an approximate 3.5-fold increase. Blakeslee et al. (2003) noted that, for their observed cluster at $z = 1.24$, deriving the scatter without reference to morphology increases the CMR scatter three- to four-fold. A similar increase can be estimated from the study by van Dokkum et al. (2001) of a cluster at $z = 1.27$ (see their fig. 3).

Fig. 10 indicates how much of the progenitor set of present-day cluster ellipticals is composed of fully formed ellipticals at any given redshift. It becomes clear from Fig. 10 that, if we look solely at the elliptical progenitors of present-day cluster ellipticals, we sample a progressively thinner fraction of the progenitor set at higher redshift. Although restricting ourselves to this subset of progenitors *seems* to give a CMR that maintains its slope and scatter with redshift (Fig. 6), an *elliptical-only* CMR can be used to constrain the SFH of only the part of the stellar mass in present-day cluster ellipticals that is contained *solely* in early-type systems at any given redshift. However, since the subset of elliptical progenitors is *not representative of all*

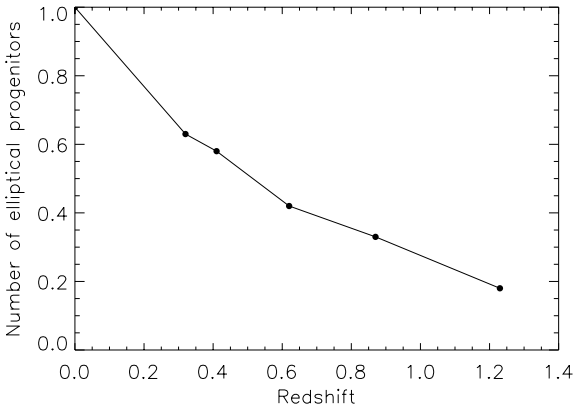

Figure 10. The number of fully formed, monolithically evolving elliptical progenitors of present-day cluster ellipticals at a given redshift. These progenitors do not undergo any further mergers, although quiescent star formation continues to $z = 0$. The remaining mass in the progenitor set is hosted by late-type systems.

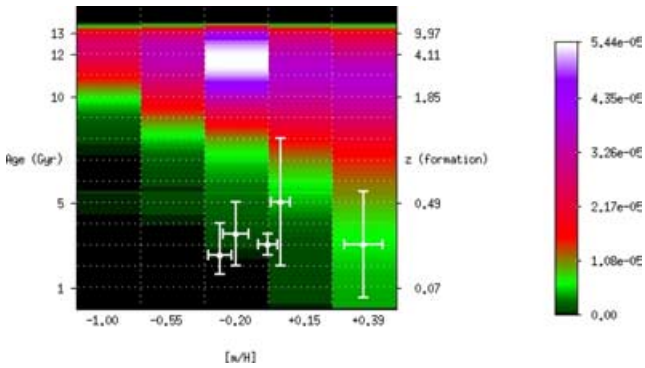

Figure 11. (See electronic journal for colour version) Predicted distribution of stellar mass contained in cluster ellipticals. Overplotted are observations of young globular clusters. From left to right: Larsen et al. (2003), Strader et al. (2003), Goudfrooij et al. (2001), Kissler-Patig et al. (2002) and Yi et al. (2004). The key indicates the mass fractions corresponding to the colours used in the plot.

the stellar material at the present day, we cannot use the evolution of an elliptical-only CMR to constrain the SFH of the entire stellar mass of present-day cluster ellipticals.

Figs 6, 9 and 10 show that the merger paradigm does indeed expect to have fully formed elliptical galaxies (and therefore a red sequence) evolving passively at redshifts where CMR observations have been conducted. However, the elliptical-only CMR at high redshift does not correspond to the elliptical-only CMR at the present day, and comparisons between the two give a heavily biased picture of the star formation history of elliptical galaxies and has serious implications for the ability of the CMR to discriminate between the monolithic collapse and hierarchical merger paradigms. In essence, the quantity (in this case the elliptical-only CMR) that is being used to discriminate between the two formation models is no longer model-independent and therefore loses its usefulness as a discriminant.

6 SUMMARY AND CONCLUSIONS

We have used a semi-analytical hierarchical galaxy formation model to investigate the existence and evolution of the CMR of elliptical galaxies in cluster environments. Our analysis shows that, by constructing a CMR purely out of early-type systems, the predicted relation agrees well with local observations (after the fixed-aperture bias has been corrected) and with observations at all redshifts in the range $0 < z < 1.27$. Secondly, we have used our analysis to quantify the issue of progenitor bias and construct the CMR that could be expected if we could identify all progenitor systems at high redshift that would eventually form part of a present-day cluster elliptical. We have also shown that the scatter in this *all-progenitor* CMR is consistent with the scatter derived, without reference to morphology, in cluster CMR studies at high redshift. Thirdly, we have suggested that the elliptical-only CMR is not a useful discriminant between the monolithic and merger formation scenarios since it is significantly biased towards the monolithic picture. Although the merger paradigm satisfies the elliptical-only CMR in any case and expects to have a monolithically evolving red sequence at high redshift, restricting our studies to early-type systems does not provide meaningful information about the true star formation history of all the stellar mass that is found today in cluster ellipticals.

The debate regarding these two competing theories of elliptical galaxy formation still remains an open one. Although there is clear evidence of interactions, mergers and recent star formation in early-type systems, a possible caveat is the inability of the merger paradigm to satisfy the high [Mg/Fe] ratios observed in luminous ellipticals (e.g. Trager et al. 2000a). These supersolar abundance ratios indicate a lack of enrichment from Type Ia supernovae, thereby constraining the duration of star formation and gas infall to timescales shorter than about 1 Gyr (e.g. Matteucci & Recchi 2001; Ferreras & Silk 2003). While the CMR has been used as an indirect tool for constraining the star formation history of cluster ellipticals, more direct sources of evidence may be required. If the stellar mass in cluster ellipticals did indeed form at $z \gg 1$, then we should not find any traces of star formation after this epoch, which in a ΛCDM universe corresponds to an age of approximately 10 Gyr. The merger models do of course predict star formation right up to the present day and one could assume that at least a small fraction of the resultant stellar mass could be locked up in globular clusters, which are the faintest stellar aggregations that can be accessed observationally.

Fig. 11 shows the bulk distribution of stellar mass in present-day cluster ellipticals predicted by the hierarchical merger paradigm. One can treat this as a probability distribution of stellar mass, with the highest intensity areas (see key) indicating ages and metallicities where most of the stellar mass is likely to be found. The crucial difference between this model distribution and a distribution based on the monolithic collapse model is the presence of *young stars*. Indeed, we find that observations of young globular clusters have been made in elliptical galaxies by a variety of authors (Goudfrooij et al. 2001; Kissler-Patig, Brodie & Minniti 2002; Larsen et al. 2003; Strader et al. 2003; Yi et al. 2004). We indicate these observations in Fig. 11. The five data points with error bars in Fig. 11 show the age–metallicity properties of *young* globular cluster populations derived in these studies. Note that the data points represent young globular clusters *only*, and are not representative of all the clusters found in these galaxies. To conclude, we suggest that it seems increasingly likely that the monolithic collapse picture may simply be a subset of the merger paradigm and that the dominant mechanism for the formation of elliptical galaxies is through the merging of late-type progenitors.

ACKNOWLEDGMENTS

We are indebted to the referee, Richard Bower, for numerous suggestions and comments which significantly improved the quality

of this paper. We warmly thank Jeremy Blaizot, Roger Davies, Joseph Silk and Sadegh Khochfar for their careful reading of this manuscript and many useful discussions. We also thank Seok-Jin Yoon for constructive remarks related to this work. SK acknowledges PPARC grant PPA/S/S/2002/03532. This research has been supported by PPARC Theoretical Cosmology Rolling Grant PPA/G/O/2001/00016 (to SKY) and has made use of Starlink computing facilities at the University of Oxford.

REFERENCES

Baum W. A., 1959, PASP, 71, 106
Beers T. C., Flynn K., Gebhardt K., 1990, AJ, 100, 32
Bernardi M. et al., 2003, AJ, 125, 1882
Blakeslee J. P. et al., 2003, ApJ, 596, L143
Bower R. G., Lucey J. R., Ellis R., 1992, MNRAS, 254, 589 (BLE92)
Bower R. G., Kodama T., Terlevich A., 1998, MNRAS, 299, 1193
Butcher H., Oemler A., 1984, ApJ, 285, 426
Caldwell N., Rose J. A., Concannon K. D., 2003, AJ, 125, 2891
Cole S., Lacey C. G., Baugh C. M., Frenk C. S., 2000, MNRAS, 319, 168
Couch W. J., Barger A. J., Smail I., Ellis R. S., Sharples R. M., 1998, ApJ, 497, 188
De Propris R. et al., 2004, astro-ph/0411646
de Vaucouleurs G., 1961, ApJS, 5, 233
Devriendt J. E. G., Guiderdoni B., Sadat R., 1999, A&A, 350, 381
Dressler A., 1980, ApJ, 236, 351
Dressler A. et al., 1997, ApJ, 490, 577
Ellingson E., Lin H., Yee H. K. C., Carlberg R. G., 2001, ApJ, 547, 609
Ellis R. S., Smail I., Dressler A., Couche W. J., Oemler A. J., Butcher H., Sharples R. M., 1997, ApJ, 483, 582
Ferreras I., Silk J., 2003, MNRAS, 344, 455
Fioc M., Rocca-Volmerange B., 1999, A&A, 351, 869
Franceschini A., Silva L., Fasano G., Granato L., Bressan A., Arnouts S., Danese L., 1998, ApJ, 506, 600
Franx M., Illingworth G., Heckman T., 1989, AJ, 98, 538
Gladders M. D., Lopez-Cruz O., Yee H. K. C., Kodama T., 1998, ApJ, 501, 571
Goudfrooij P., Mack J., Kissler-Patig M., Meylan G., Minniti D., 2001, MNRAS, 322, 643
Hatton S., Devriendt J. E. G., Ninin S., Bouchet F. R., Guiderdoni B., Vibert D., 2003, MNRAS, 343, 75
Kauffmann G., Charlot S., 1998, MNRAS, 297, L23
Kauffmann G., White S. D. M., Guiderdoni B., 1993, MNRAS, 264, 201
Kauffmann G., Charlot S., White S. D. M., 1996, MNRAS, 283, L117
Kennicutt R. C., 1983, ApJ, 272, 54
Khochfar S., Burkert A., 2003, ApJ, 597, L117
Kissler-Patig M., Brodie J. P., Minniti D., 2002, A&A, 391, 441
Kodama T., Arimoto N., 1997, A&A, 320, 41
Larsen S. S., Brodie J. P., Beasley M. A., Forbes D. A., Kissler-Patig M., Kuntschner H., Puzia T. H., 2003, ApJ, 585, 767
Larson R. B., 1974, MNRAS, 166, 385
McClure R. D., van den Bergh S., 1968, AJ, 73, 1008
Magorrian J. et al., 1998, AJ, 115, 2285
Margoniner V. E., de Carvalho R. R., Gal R. R., Djorgovski S. G., 2001, ApJ, 548, L143
Matteucci F., Recchi S., 2001, ApJ, 558, 351
Peletier R. F., Davies R. L., Illingworth G. D., Davis L. E., Cawson M., 1990, AJ, 100, 1091
Pimbblet K. A., Smail I., Kodama T., Couch W. J., Edge A. C., Zabludoff A. I., O'Hely E., 2002, MNRAS, 331, 333
Prugniel P., Simien F., 1996, A&AS, 309, 749
Sandage A., Vishvanathan N., 1977, ApJ, 203, 707
Sandage A., Vishvanathan N., 1978, ApJ, 225, 742
Schade D., Lilly S. J., Crampton D., Hammer F., Le Fevre O., Tresse L., 1995, ApJ, 451, L1
Scodeggio M., 2001, AJ, 121, 2413
Shioya Y., Bekki K., 1998, ApJ, 504, 42
Somerville R. S., Primack J. R., 1999, MNRAS, 310, 1087
Stanford S. A., Eisenhardt P. R. M., Dickinson M., 1998, ApJ, 492, 461
Strader J., Brodie J. P., Schweizer F., Larsen S. S., Seitzer P., 2003, AJ, 125, 626
Terlevich A. I., Caldwell N., Bower R. G., 2001, MNRAS, 326, 1547
Trager S. C., Faber S. M., Worthey G., González J. J., 2000a, AJ, 119, 1645
Trager S. C., Faber S. M., Worthey G., González J. J., 2000b, AJ, 120, 165
Tsujimoto T., Yoshii Y., Nomoto K., Matteucci F., Thielemann F., Hashimoto M., 1997, ApJ, 483, 228
van den Bosch F. C., 2002, MNRAS, 331, 98
van Dokkum P. G., Franx M., 2001, ApJ, 553, 90
van Dokkum P. G., Franx M., Kelson D. D., Illingworth G. D., 1998, ApJ, 504, L17
van Dokkum P. G., Franx M., Fabricant D., Kelson D. D., Illingworth 1999, ApJ, 520, L95
van Dokkum P. G., Franx M., Fabricant D., Illingworth G. D., Kelson D. D., 2000, ApJ, 541, 95
van Dokkum P. G., Stanford S. A., Holden B. P., Eisenhardt P. R., Dickinson M., Elston R., 2001, ApJ, 552, L101
Yi S. K., 2003, ApJ, 582, 202
Yi S. K., Peng E., Ford H., Kaviraj S., Yoon S.-J., 2004, MNRAS, 349, 1493

This paper has been typeset from a TEX/LATEX file prepared by the author.